

Supporting Information

Chromosulfine, a Novel Cyclopentachromone Sulfide Produced by a Marine-derived Fungus after Introduction of Neomycin Resistance

Le Yi,^a Cheng-Bin Cui,^{*a} Chang-Wei Li,^a Ji-Xing Peng,^b and Qian-Qun Gu^b

^a *State Key Laboratory of Toxicology and Medical Countermeasures, Beijing Institute of Pharmacology and Toxicology, Beijing 100850, China*

^b *Key Laboratory of Marine Drugs, Chinese Ministry of Education, School of Medicine and Pharmacy, Ocean University of China, Qingdao 266003, China*

* To whom correspondence should be addressed. Email: cuib@126.com or cuib@sohu.com; Fax & Tel: 86-10-68211656.

Table of Contents

No.	Content	Page
1	Experimental section.	S3-S6
2	Physicochemical and spectroscopic data of chromosulfin (1).	S7
3	Table S1. 600 MHz ^1H and 150 MHz NMR data of 1 in $\text{DMSO-}d_6$.	S7
4	Table S2. 400 MHz ^1H NMR data (δ , J in Hz) of 1 and its 17- <i>O</i> -MTPA esters in pyridine- d_5 .	S8
5	Figure S1. DFT-optimized structures of the low-energy conformers of 1s at the B3LYP/6-31+G(d) level using a polarizable continuum model (PCM) in acetonitrile.	S9
6	Figure S2. DFT-optimized structures of the low-energy conformers of <i>ent-1s</i> at the B3LYP/6-31+G(d) level using a polarizable continuum model (PCM) in acetonitrile.	S9
7	Figure S3. HPLC-PDAD-UV analysis of the EtOAc extracts of mutant 4-30 and the parent G59 strain to detect 1 .	S10
8	Figure S4. HPLC-ESI-MS analysis of the EtOAc extracts of mutant 4-30 and the parent G59 strain to detect 1 .	S10
9	Figure S5. Positive ESI-MS spectrum of 1 .	S11
10	Figure S6. Positive HR-ESI-MS spectrum of 1 .	S11
11	Figure S7. UV spectrum of 1 in MeOH.	S11
12	Figure S8. IR spectrum of 1 (on an ATR crystal).	S12
13	Figure S9. 600 MHz ^1H NMR spectrum of 1 in $\text{DMSO-}d_6$.	S12
14	Figure S10. 600 MHz ^1H NMR spectrum of 1 in $\text{DMSO-}d_6$ after adding drops of D_2O .	S13
15	Figure S11. 150 MHz ^{13}C NMR spectrum of 1 in $\text{DMSO-}d_6$.	S13
16	Figure S12. 100 MHz ^{13}C NMR and DEPT spectra of 1 in $\text{DMSO-}d_6$.	S14
17	Figure S13. 400 MHz ^1H - ^1H COSY spectrum of 1 in $\text{DMSO-}d_6$.	S14
18	Figure S14. 400 MHz ^1H /100 MHz ^{13}C HMQC spectrum of 1 in $\text{DMSO-}d_6$.	S15
19	Figure S15. 600 MHz ^1H /150 MHz ^{13}C HMBC spectrum of 1 in $\text{DMSO-}d_6$.	S15
20	Figure S16. 600 MHz ROESY spectrum of 1 in $\text{DMSO-}d_6$.	S16
21	Figure S17. 600 MHz ^1H NMR and 1D GOESY spectra of 1 in $\text{DMSO-}d_6$.	S16

Experimental Section

General Experimental Procedures. Optical rotations were measured in an Optical Activity Limited PolAAR 3005 spectropolarimeter. ESIMS was recorded on an AB SCIEX Applied Biosystems API 3000 LC-MS spectrometer, and HRESIMS was recorded on an Agilent 6520 Q-TOF LC-MS spectrometer. UV data were acquired with a Varian CARY300 spectrophotometer. IR spectra were recorded on a Bruker Tensor-27 infrared spectrophotometer. CD data were measured on a Bio-Logic Science MOS450 CD spectrometer. NMR spectra were acquired on a JEOL JNM-GX 400 (400 MHz for ^1H /100 MHz for ^{13}C) or Bruker-600 (600 MHz for ^1H /150 MHz for ^{13}C) NMR spectrometer. Thin-layer chromatography (TLC) was performed using precoated silica gel GF₂₅₄ plates (0.25-mm thickness, Yantai Chemical Industrial Institute, China), and the TLC spots were detected under sunlight and UV light (254 and 365 nm) or by using Vaughan's reagent.¹ Column chromatography was performed using Silica gel H (200–300 mesh, Yantai Chemical Industrial Institute, Yantai, China), YMC*GEL® ODS-A-HG (12 nm S-50 μm , YMC Co., Ltd., Kyoto, Japan), or Sephadex™ LH-20 (GE Healthcare, Uppsala, Sweden). HPLC was performed on a Waters HPLC system equipped with a Waters 600 controller, a Waters 600 pump, a Waters 2414 refractive index detector, and a Waters 2996 (for analytical HPLC) or 2998 (for preparative HPLC) photodiode array detector using Waters Empower™ software. Venusil MP C₁₈ (5 μm , 100 Å, 4.6 mm × 250 mm; Agela Technologies, Tianjin, China) and Capcell Pak C₁₈ (MG II, 4.6 mm × 250 mm; Shiseido Co., Ltd., Tokyo, Japan) columns were used for analytical HPLC, and a Capcell Pak C₁₈ (MG II, 10 mm × 250 mm; Shiseido Co., Ltd., Tokyo, Japan) column was used for semi-preparative HPLC. Optical density was measured on a VersaMax-BN03152 microplate reader (Molecular Devices, Silicon Valley, CA, USA). Cell morphology was examined using an AE31 EF-INV inverted microscope (Motic China Group Co., Ltd., Xiamen, Fujian, China).

Cell Lines and Reagents. The human chronic myelogenous leukemia K562 cell line was provided by Lili Wang (Beijing Institute of Pharmacology and Toxicology, Beijing, China). The human cell lines acute promyelocytic leukemia HL-60, cervical cancer HeLa, gastric adenocarcinoma BGC-823, and breast cancer MCF-7 were provided by Wenxia Zhou (Beijing Institute of Pharmacology and Toxicology). Fetal bovine serum was purchased from Tianjin Hao Yang Biological Manufacture Co., Ltd. (Tianjin, China). RPMI-1640 medium (lot no. 1403238) and MTT (lot no. 0793) were purchased from Gibco (Grant Island, NY, USA) and Amresco (Solon, OH, USA), respectively. Streptomycin (lot no. 071104) and penicillin (lot no. X11303302) were purchased from North China Pharmaceutical Group Corporation, Beijing, China. 5-Fluorouracil (5-FU, lot no.5402) was purchased from Aladdin Chemistry Co., Ltd. (Shanghai, China).

Fungal Strains. The parent fungal strain *Penicillium purpurogenum* G59 used as the control in the present study was isolated from a soil sample collected at the tideland of Bohai Bay around Lūjūhe in

the Tanggu district of Tianjin, China in September 2004.² It was identified by Prof. Liang-Dong Guo of the Institute of Microbiology of the Chinese Academy of Sciences in China. This strain has been deposited in the China General Microbiological Culture Collection Center under the accession number CGMCC No. 9721. The mutant 4-30 used as the producing strain in the present study is a neomycin-resistant mutant of the marine-derived fungus *P. purpurogenum* G59. This mutant was selected by our group in a previous study by treating G59 spores with 6.7 mg/mL neomycin in 67% DMSO at 4 °C for 7 days.³ This mutant strain has been deposited at the China General Microbiological Culture Collection Center under the accession number CGMCC No. 11655.

Fermentation and Extraction. Spore suspensions of the mutant 4-30 and the parent G59 strain were prepared using fresh spores according to the procedure reported previously.⁴ The spore density of the suspensions was adjusted to a value of 1.24 by monitoring the OD at 600 nm on a VersaMax-BN03152 microplate reader.

Producing fermentation of the mutant 4-30 was conducted in 75 500-mL Erlenmeyer flasks, each containing 80 g of rice. Distilled water (150 mL) was added to each flask, and the contents were soaked overnight before autoclaving at 121 °C for 30 min. After cooling the flasks to room temperature, an aliquot (200 µL) of the mutant 4-30 spore suspension was inoculated into each flask and incubated at 28 °C for 80 days. The fermented material was extracted with 250 mL of 80% (v/v) aqueous acetone by ultrasonication for 4 h. After filtration, the remaining solid substances in each flask were combined and extracted three times with acetone (3 × 15 L). The aqueous acetone solutions were combined and evaporated under reduced pressure to remove the acetone, and the remaining water layer (8 L) was extracted three times with equal volumes of EtOAc (3 × 8 L) to obtain an EtOAc extract (99.9 g). This extract inhibited K562 cells with an inhibition rate (IR%) of 51.8% at 100 µg/mL. Compound **1** was isolated from this extract. Simultaneously, the parent G59 strain was fermented and extracted in the same manner. One 500-mL Erlenmeyer flask was used to obtain an EtOAc extract (1.2 g). The extract did not inhibit K562 cells (an IR% of 5.9% at 100 µg/mL). This extract was used as the negative control in the chromatography of the mutant 4-30 extract for tracking the production of **1** by the mutant. The EtOAc extracts of the mutant and the parent strains were used in HPLC-photo diode array (PDAD)-UV and HPLC-ESI-MS analyses to detect **1**.

Isolation of 1. The EtOAc extract (99.8 g) of the mutant 4-30 was fractionated by vacuum liquid chromatography on a silica gel column (silica gel, 800 g; bed, 8.5 cm × 35 cm) by stepwise elution with b.p. 60-90 °C petroleum ether (P)–dichloromethane (D)–methanol (M) to obtain thirteen fractions: **Fr-1** (17.7 g, eluted by P → PD 1:2), **Fr-2** (12.2 g, eluted by PD 1:2 → 1:5), **Fr-3** (3.7 g, eluted by D), **Fr-4** (1.9 g, eluted by D → DM 99:1), **Fr-5** (3.9 g, eluted by DM 99:1 → 98:2), **Fr-6** (9.8 g, eluted by DM 98:2 → 97:3), **Fr-7** (9.7 g, eluted by DM 97:3 → 96:4), **Fr-8** (5.3 g, eluted by DM 96:4 → 95:5), **Fr-9**

(6.8 g, eluted by DM 95:5 → 90:10), **Fr-10** (8.4 g, eluted by DM 90:10 → 85:15), **Fr-11** (6.2 g, eluted by DM 85:15 → 70:30), **Fr-12** (5.8 g, eluted by DM 70:30 → 50:50), and **Fr-13** (8.1 g, eluted by DM 50:50). The fractions **Fr-6**, **Fr-7**, **Fr-8**, **Fr-9** and **Fr-10** inhibited K562 cells with IR% values of 72.9%, 73.3%, 68.4%, 60.4% and 74.1%, respectively, at 100 µg/mL. TLC analysis and direct comparison with the parent G59 extract indicated that **Fr-10** (8.4 g) contained **1**. Thus, **Fr-10** (8.4 g) was separated on a Sephadex LH-20 column (bed 6 cm × 40 cm) and eluted with 95% alcohol to obtain six fractions, **Fr-10-1** to **Fr-10-6**, in order of elution. Metabolite **1** was detected in **Fr-10-4** by TLC. Further separation of **Fr-10-4** (0.6 g) by semi-preparative HPLC (column: Capcell Pak C₁₈, MG II, 10 mm × 250 mm; MeOH–H₂O 55:45, flow rate: 2.5 mL/min; detection wavelength: 200 nm) yielded **1** (8 mg, *t_R* = 36.4 min) as a brown amorphous powder from MeOH.

Preparation of (S)- and (R)-MTPA Esters of 1. Compound **1** (0.3 mg, 0.71 µmol) was reacted with (S)- or (R)-MPTA Cl (1 µL, 5.34 µmol) in 0.2 mL of anhydrous pyridine-*d*₆ at room temperature in NMR tubes. The esterification reaction was monitored based on the ¹H NMR spectra of the 17-*O*-(S)-MPTA and 17-*O*-(R)-MPTA monoesters, **1a** and **1b**, respectively. The monoesters were obtained without purification after reaction with (S)- and (R)-MPTA Cl for 4 days and 5 h, respectively.

HPLC-PDAD-UV and HPLC-ESI-MS Analysis. The EtOAc extracts of the mutant 4-30 and the parent G59 strains were dissolved in MeOH to prepare sample solutions at 10 mg/mL for HPLC-PDAD-UV and HPLC-ESI-MS. Crude **1** in MeOH at 1 mg/mL was used as the reference standard in the HPLC-PDAD-UV analysis. The HPLC-PDAD-UV analysis was performed on a Venusil MP C₁₈ column (5 µm, 100 Å, 4.6 mm × 250 mm; Agela Technologies, Tianjin, China) using the Waters HPLC equipment described in the General Experimental Procedures. The sample solutions and standard solutions were filtered using 0.22-µm pore membrane filters, and 10 µL of the solutions was injected into the column. The elution was performed using a linear gradient of MeOH-H₂O (20% MeOH at initial time 0 min → 100% MeOH at 60 min → 100% MeOH at 90 min; flow rate, 0.6 mL/min). The acquired photodiode array data were processed using the Waters Empower™ software to obtain the targeted HPLC-PDAD-UV data. Compound **1** was eluted as a peak with a *t_R* of 49.35 min and was detected based on both its *t_R* and the UV spectra. Compound **1** was detected in the mutant 4-30 extract but not in the G59 extract based on retention time and the UV spectra. HPLC-ESI-MS analysis was performed on a LC-MS equipped with an Agilent 1100 HPLC system and an AB Sciex API 3000 LC-MS/MS system with AB Sciex Analyst 1.4 software (AB SCIEX, Framingham, USA). HPLC was conducted on the same Venusil MP C₁₈ column (5 µm, 100 Å, 4.6 mm × 250 mm; Agela Technologies, Tianjin, China) under identical conditions as the HPLC-PDAD-UV analysis. The mass detector was set to scan a range from *m/z* 150 to 1,500 in both positive and negative modes. The acquired data were processed using Analyst 1.4 software to obtain the targeted HPLC-ESI-MS data. The *pseudo*-molecular

ions of **1** appeared as peaks with t_R values of 44.0–45.0 min in positive and negative modes. The retention times were slightly shorter than those in the HPLC-PDAD-UV analysis because of the shorter flow length from the outlet of the HPLC column to the inlet of MS in the HPLC-ESI-MS. Compound **1** was detected by selective ion monitoring (m/z : 425 $[M+H]^+$, 447 $[M+Na]^+$ and 423 $[M-H]^-$ for **1**) of both the extracted ion chromatograms and the related MS spectra.

TDDFT Electronic CD (ECD) Calculation of **1s and *ent-1s*.** Conformational searches were performed employing the ‘systematic’ procedure implemented in Spartan’14 using MMFF (Merck molecular force field).⁵ All MMFF minima were re-optimized using DFT calculations at the B3LYP/6-31+G(d) level with the Gaussian 09 program.⁶ The geometry was optimized starting from various initial conformations with vibrational frequency calculations confirming the presence of minima. The DFT calculations were performed on the lowest-energy conformations (> 5% population) of each configuration using 30 excited states and a polarizable continuum model (PCM) in acetonitrile for **1s** and *ent-1s*, respectively. The ECD spectra were generated using the program SpecDis by applying a Gaussian band shape with a 0.35-eV width from dipole-length rotational strengths.⁷ The dipole velocity forms yielded negligible differences. The ECD spectra of the conformers were combined using Boltzmann weighting; the lowest-energy conformations accounting for approximately 94% of the weights. The calculated spectrum was red-shifted by 3 nm to facilitate comparison with the experimental data.

MTT Assay. The MTT assay was performed according to the procedure previously described.¹⁻⁴ Exponentially growing K562, HL-60, HeLa, MCF-7 and BGC-823 cells were treated with the samples at 37 °C for 24 h. The assay was performed in triplicate, and the OD value was determined at 570 nm on a VersaMax-BN03152 plate reader. The IR% was calculated using the mean value of the OD according to the formula: $IR\% = (OD_{\text{control}} - OD_{\text{sample}}) / OD_{\text{control}} \times 100\%$. The IC_{50} for compound **1** was obtained from its IR% values at different concentrations. The EtOAc extracts and fractions in MeOH at 10.0 mg/mL, **1** and 5-FU in 20% (v/v) aqueous DMSO at 10.0 mg/mL, and serial dilutions of the 20% (v/v) aqueous DMSO solution of **1** at 10.0 mg/mL were used in the MTT assay. 5-FU was used as the positive control. MeOH and 20% (v/v) aqueous DMSO solution were used as relevant blank controls.

References

1. (a) Wu, C.-J.; Li, C.-W.; Cui, C.-B. *Mar. Drugs* **2014**, *12*, 1815–1838. (b) Xia, M.-W.; Cui, C.-B.; Li, C.-W.; Wu, C.-J. *Mar. Drugs* **2014**, *12*, 1545–1568.
2. Tian, C.-K.; Cui, C.-B.; Han, X.-X. *J. Int. Pharm. Res.* **2008**, *35*, 401–405.
3. Wu, C.-J.; Yi, L.; Cui, C.-B.; Li, C.-W.; Wang, N.; Han, X. *Mar. Drugs* **2015**, *13*, 2465–2487.
4. (a) Chai, Y.-J.; Cui, C.-B.; Li, C.-W.; Wu, C.-J.; Tian, C.-K.; Hua, W. *Mar. Drugs* **2012**, *10*, 559–582. (b) Fang, S.-M.; Cui, C.-B.; Li, C.-W.; Wu, C.-J.; Zhang, Z.-J.; Li, L.; Huang, X.-J.; Ye, W.-C. *Mar. Drugs* **2012**, *10*, 1266–1287.
5. *Spartan’14*; Wavefunction Inc.: Irvine, CA, USA, 2013.
6. *Gaussian 09*, Revision A.01; Gaussian Inc.: Wallingford, CT, USA, 2009.

Physicochemical and Spectroscopic Data of Chromosulfine (1)

Chromosulfine (1): a brown amorphous powder (from MeOH), $[\alpha]_D^{25}$ -14.9 (*c* 0.5, MeOH). Positive ESIMS *m/z*: 425 [M + H]⁺, 442 [M + NH₄]⁺, 447 [M + Na]⁺, 463 [M + K]⁺, 871 [2M + Na]⁺. Positive HRESIMS *m/z*: measured 447.0728 [M + Na]⁺, calculated for C₁₉H₂₀NaO₉S 447.0726; measured 871.1570 [2M + Na]⁺, calculated for C₃₈H₄₀NaO₁₈S₂ 871.1554. UV λ_{\max} nm (log ϵ) in MeOH: 202 (4.28), 228 (4.19), 238 (4.19), 258 (shoulder peak, 4.04), and 323 (3.56). IR ν_{\max} cm⁻¹ (diamond ATR crystal): 3274 (OH), 2930, 2855 (CH₃/CH₂/CH), 1737 (ester carbonyl), 1656 (conjugated carbonyl), 1624, 1604, 1491 (Ar-ring), 1454, 1365, 1262, 1208, 1147, 1126, 1073, 1028, 954, 827, 817, 780. CD (MeOH) $\Delta\epsilon$ (nm): +3.95 (208.0), +1.54 (220.5), +2.70 (232.0), +2.35 (240.5), +2.95 (255.0), 0 (269.5), -1.36 (283.0), -0.96 (294.0), -1.45 (317.0), -0.08 (369.5), 0 (426.5). 600 MHz ¹H and 150 MHz ¹³C NMR data in DMSO-*d*₆: Table S1.

Table S1. 600 MHz ¹H and 150 MHz ¹³C NMR data of 1 in DMSO-*d*₆.

Position	δ_C ^a	δ_H ^a (J in Hz)	COSY ^b	NOE ^c	HMBC ^d
1	172.2 s	—	—	—	—
2	79.4 s	—	—	—	—
3	51.0 d	3.98 dd (9.0, 8.1)	H ₂ -4	H α -4, H β -4, H ₃ -15, H ₂ -16, H-17, H ₃ -19	C-1, 2, 4, 13, 16
4	37.5 t	H α 3.06 dd (17.4, 9.0) H β 3.46 dd (17.4, 8.1)	H-3, H β -4 H-3, H α -4	H-3, H β -4 H-3, H α -4	C-3, 5, 6, 13 C-2, 3, 5, 13
5	121.6 s	—	—	—	—
6	178.2 s	—	—	—	—
7	108.2 s	—	—	—	—
8	159.9 s	—	—	—	—
9	112.4 d	6.94 br s	H-11, H ₃ -14	H ₃ -14	C-6, 7, 8, 11, 14
10	147.3 s	—	—	—	—
11	108.0 d	6.96 br s	H-9, H ₃ -14	H ₃ -14	C-6, 7, 9, 12, 14
12	156.5 s	—	—	—	—
13	171.8 s	—	—	—	—
14	21.7 q	2.38 3H, br s	H-9, H-11	H-9, H-11	C-9, 10, 11
15	52.5 q	3.71 3H, s	—	—	C-1
16	34.7 t	H α 2.86 dd (13.7, 5.1) H β 2.78 dd (13.7, 6.9)	H β -16, H-17 H α -16, H-17	H-3, H-17, H ₃ -15, H ₃ -19 H-3, H-17, H ₃ -15, H ₃ -19	C-3, 17, 18 C-3, 17, 18
17	70.7 d	4.22 dd (6.9, 5.1)	H ₂ -16	H-3, H ₂ -16, H ₃ -15, H ₃ -19	C-16, 18
18	172.7 s	—	—	—	—
19	51.6 q	3.66 3H, s	—	H-3, H ₂ -16, H-17, 17-OH	C-18
2-OH	—	5.83 br s	—	—	—
8-OH	—	12.34 br s	—	—	—
17-OH	—	5.95 br s	—	H ₃ -19	C-7, 8, 9

^a The δ_C/δ_H values were recorded using the solvent DMSO-*d*₆ signals (δ_C 39.52/ δ_H 2.50) as references and the signals were assigned on the basis of DEPT, 2D ¹H-¹H COSY, HMQC, HMBC, NOESY and 1D GOESY difference NOE experiments. ^b The numbers in each line of this column indicate the protons that correlated with the proton in the corresponding line in ¹H-¹H COSY. ^c The numbers in each line of this column indicate the protons that showed NOE correlations with the proton in the corresponding line in 2D NOESY and ROESY or 1D GOESY difference NOE experiments. A more remarkable NOE was detected on H α -4 than on H β -4 when H-3 was irradiated in the 1D GOESY difference NOE experiments, which enabled us to distinguish the H α -4 and H β -4

signals. ^d The numbers in each line of this column indicate the carbons that showed HMBC correlations with the proton in the corresponding line in HMBC experiments (optimized for the 8.3 or 5 Hz of long-range J_{CH} value).

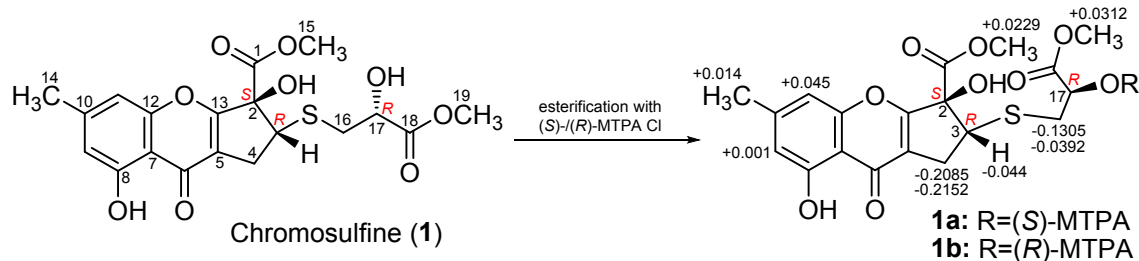


Table S2. 400 MHz ¹H NMR Data (δ , J in Hz) of **1** and its 17-*O*-MTPA Esters (**1a/1b**) in Pyridine-*d*₅.^a

Protons	1	1a	1b	$\Delta\delta = \delta_S - \delta_R$
3	4.68 dd (9.0, 7.8)	4.4202 dd (9.0, 8.5)	4.4645 dd (9.0, 8.0)	-0.0443
4 H α	3.42 dd (17.5, 9.0)	3.2030 dd (17.2, 9.0)	3.41825 dd (17.9, 9.0)	-0.21525
H β	3.55 dd (17.5, 7.8)	3.2073 dd (17.2, 8.5)	3.41585 dd (17.9, 8.0)	-0.20855
9	6.69 s	6.6999 br s	6.6987 br s	+0.0012
11	6.69 s	6.7645 br s	6.7193 br s	+0.0452
14	2.20 3H, s	2.2273 s	2.2128 s	+0.0145
15	3.90 3H, s	3.9432 s	3.9203 s	+0.0229
16	3.41 2H, d (5.5)	3.4134 2H, d (5.6)	Ha 3.54395 dd (14.7, 3.3) Hb 3.4526 dd (14.7, 8.8)	-0.13055 -0.0392
17	4.88 t (5.5)	6.0665 t (5.6)	6.0245 dd (8.8, 3.3)	+0.042
19	3.71 3H, s	3.7035 s	3.6723 s	+0.0312
2-OH	ND	ND	ND	ND
17-OH	ND	ND	ND	ND
8-OH	12.88 br s	ND	ND	ND

^a The chemical shift δ_H values were recorded using the solvent pyridine-*d*₅ signal (δ_H 8.74) as a reference. The data for **1a** and **1b** were obtained after the reaction of **1** with (*S*)-MTPA Cl for 4 days and (*R*)-MTPA Cl for 5 h at room temperature. At these times, only 17-*O*-MTPA esters were formed in the reactions with (*S*)-MTPA Cl and (*R*)-MTPA Cl. The reaction of **1** with (*S*)-MTPA Cl afforded only 17-*O*-MTPA monoesters, even at the 6th day of reaction, as detected by ¹H NMR. By contrast, both 17-*O*- and 2,17-di-*O*-MTPA esters were formed in the reaction with (*R*)-MTPA Cl, with increased amounts of the 2,17-di-*O*-MTPA ester with increased reaction time from the 1st day of the reaction. ND: not detected.

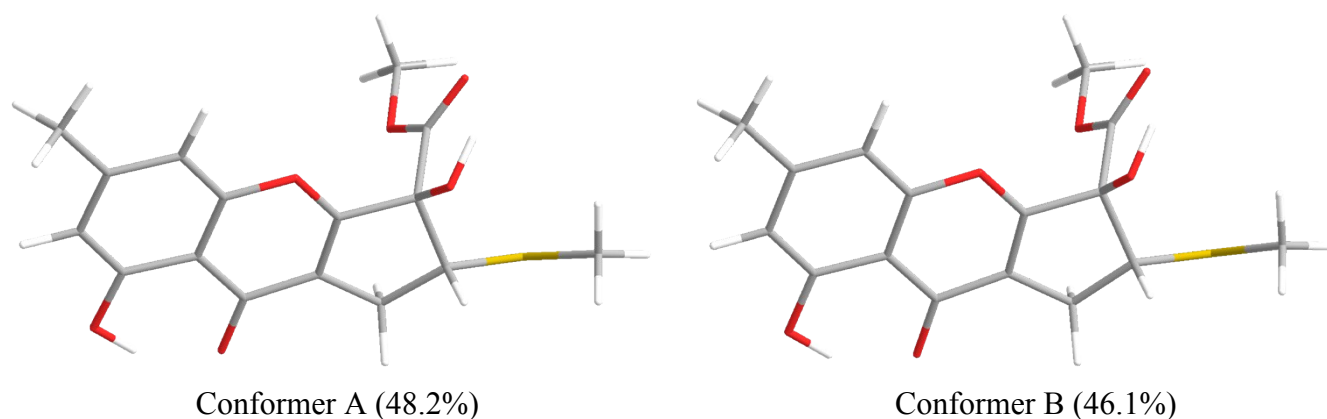


Figure S1. DFT-optimized structures of the low-energy conformers of **1s** at the B3LYP/6-31+G(d) level using a polarizable continuum model (PCM) in acetonitrile. The conformer population was calculated using the Gibbs free energy and Boltzmann population at 298 K.

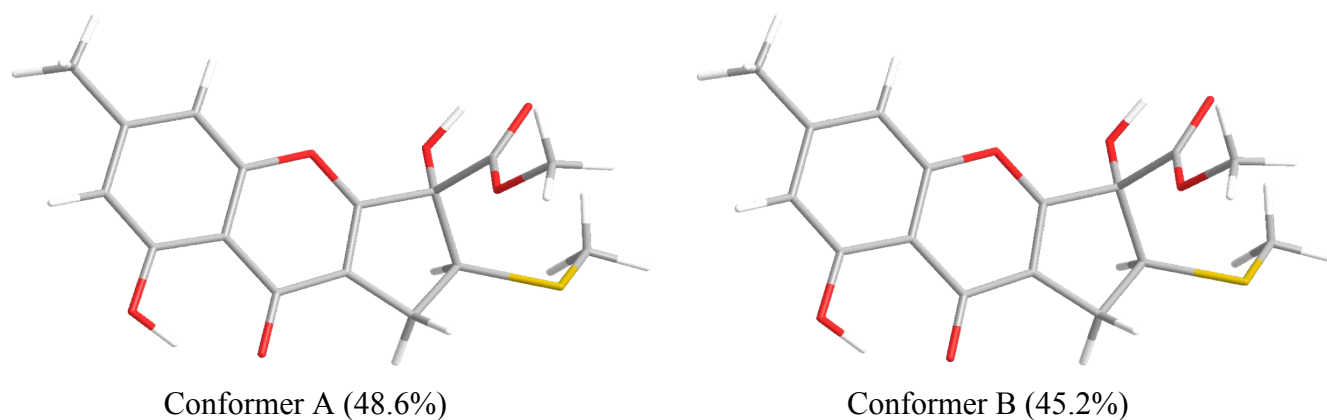
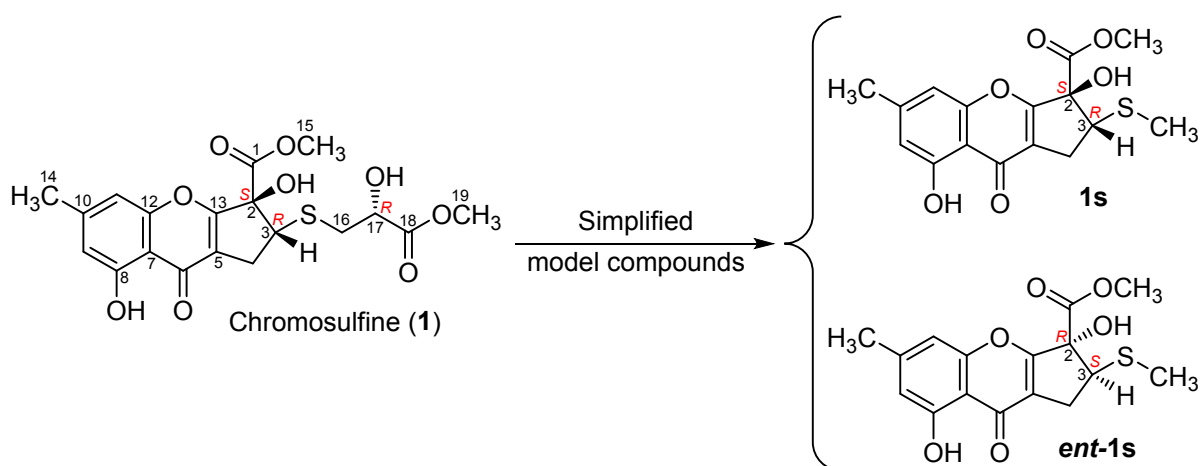
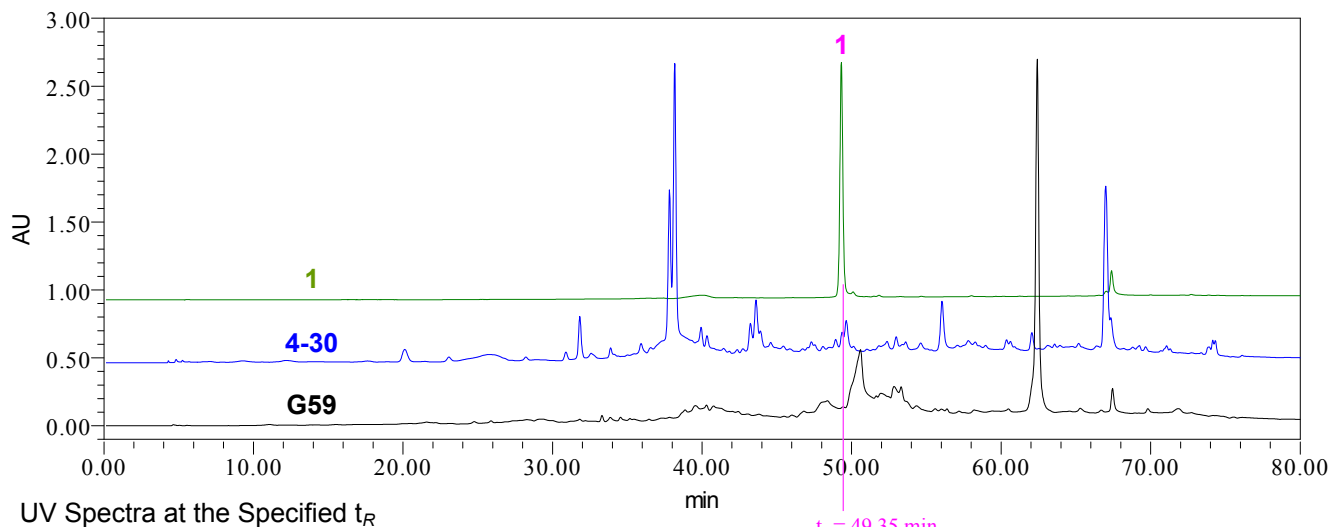


Figure S2. DFT-optimized structures of the low-energy conformers of **ent-1s** at the B3LYP/6-31+G(d) level using a polarizable continuum model (PCM) in acetonitrile. The conformer population was calculated using the Gibbs free energy and Boltzmann population at 298 K.

HPLC Profiles Detected at 240 nm



UV Spectra at the Specified t_R

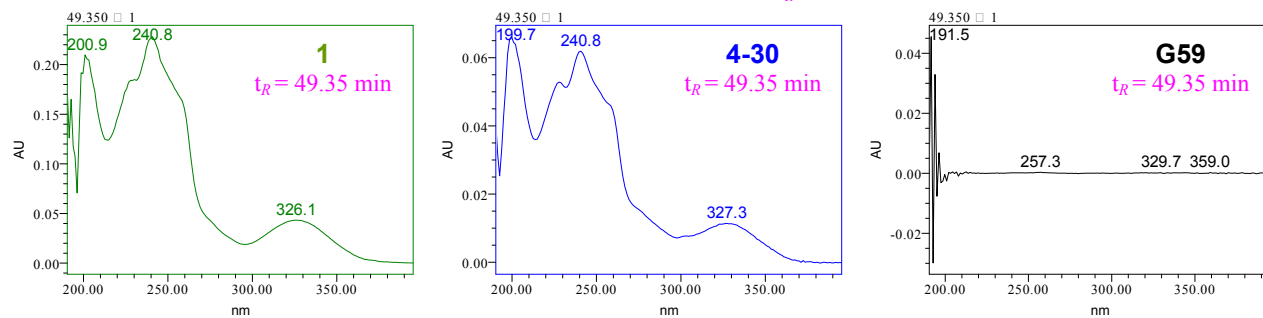


Figure S3. HPLC-PDAD-UV analysis of the EtOAc extracts of mutant 4-30 and the parent G59 strain to detect **1**.

Extracted Negative Ion Chromatograms (m/z 424.5-425.5)

ESIMS Spectra at Retention Times of 44.55-44.65 min

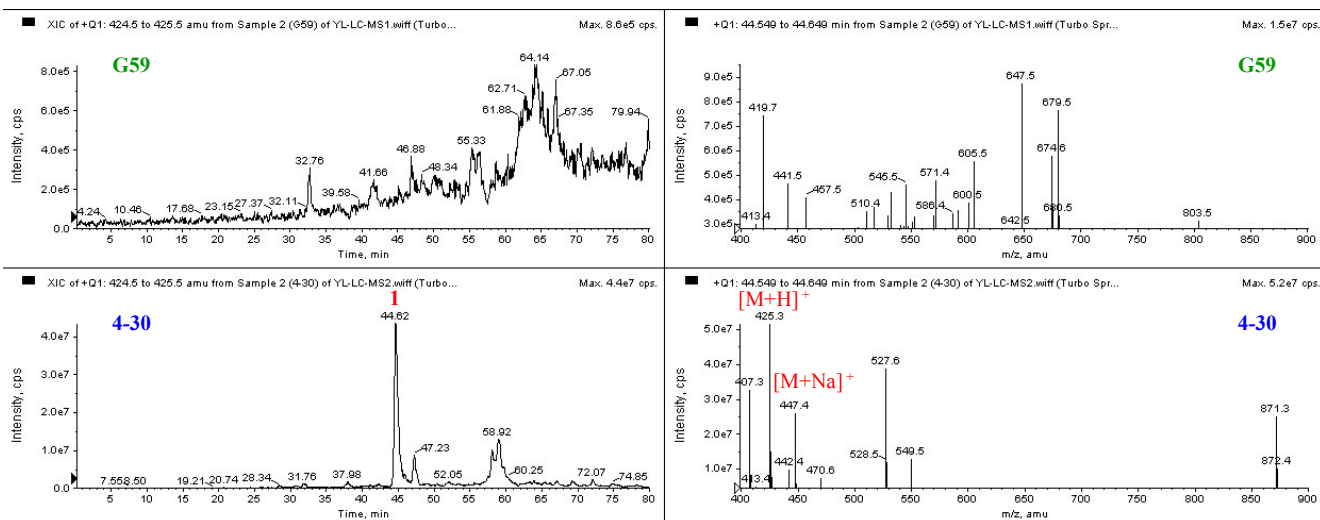


Figure S4. HPLC-ESI-MS analysis of the EtOAc extracts of the mutant 4-30 and the parent G59 strain to detect **1**.

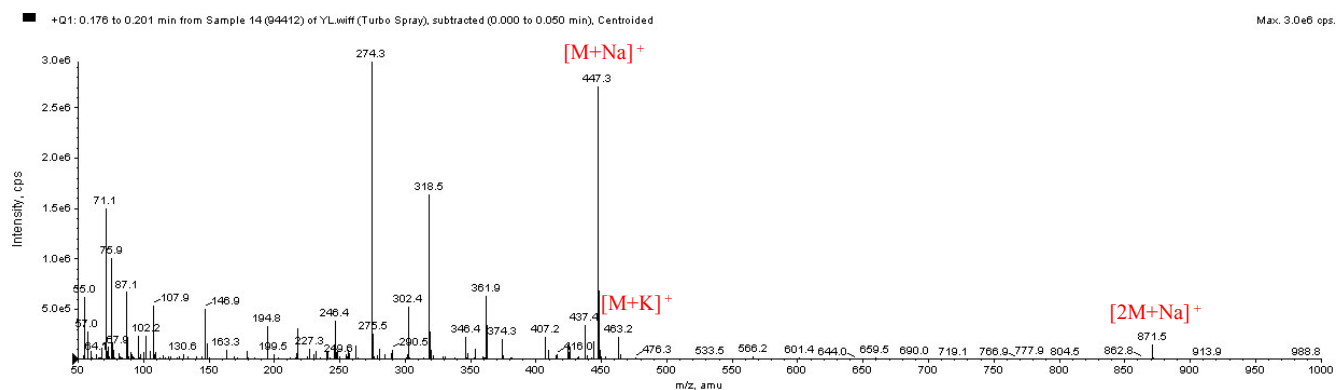


Figure S5. Positive ESI-MS spectrum of **1**.

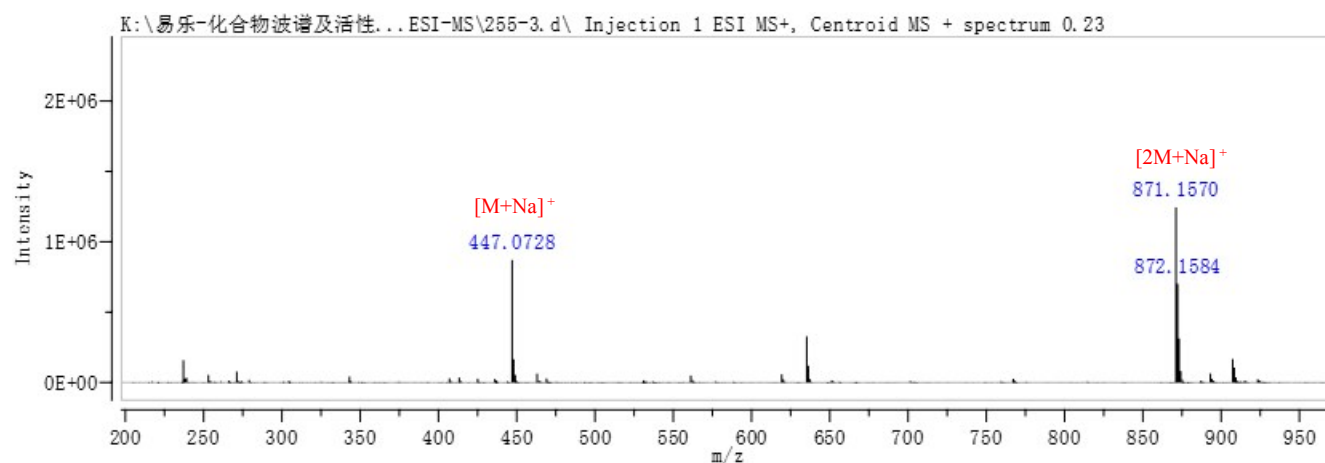


Figure S6. Positive HR-ESI-MS spectrum of **1**.

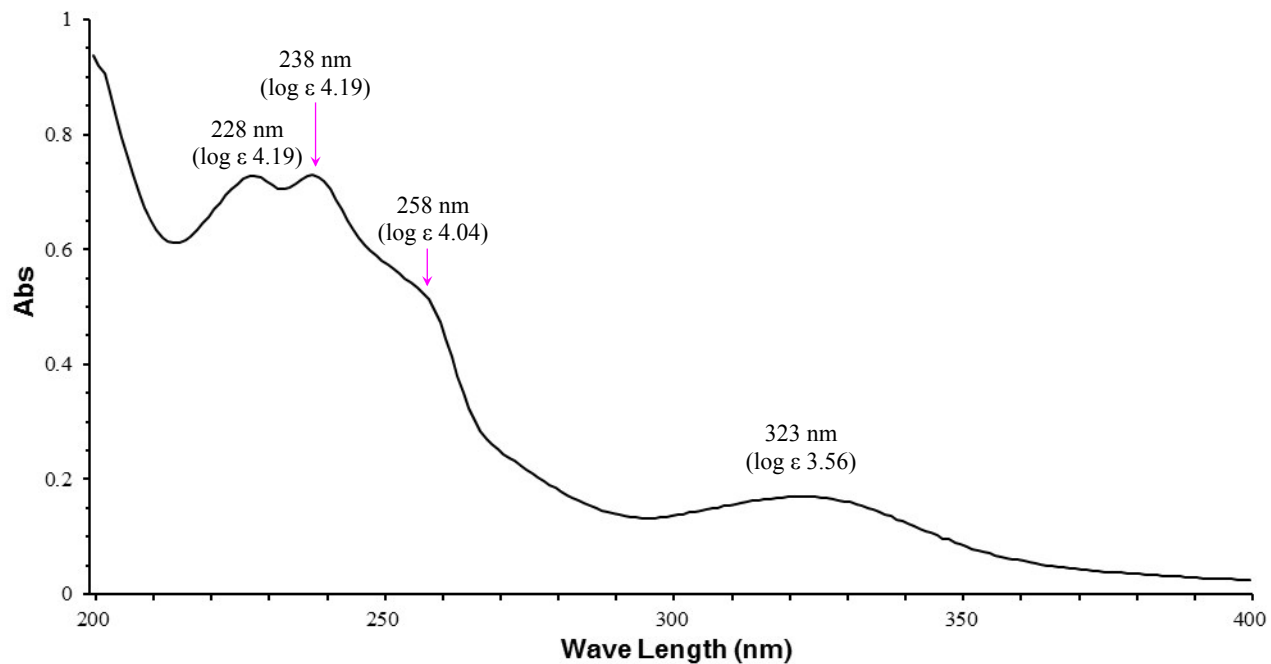


Figure S7. UV spectrum of **1** in MeOH.

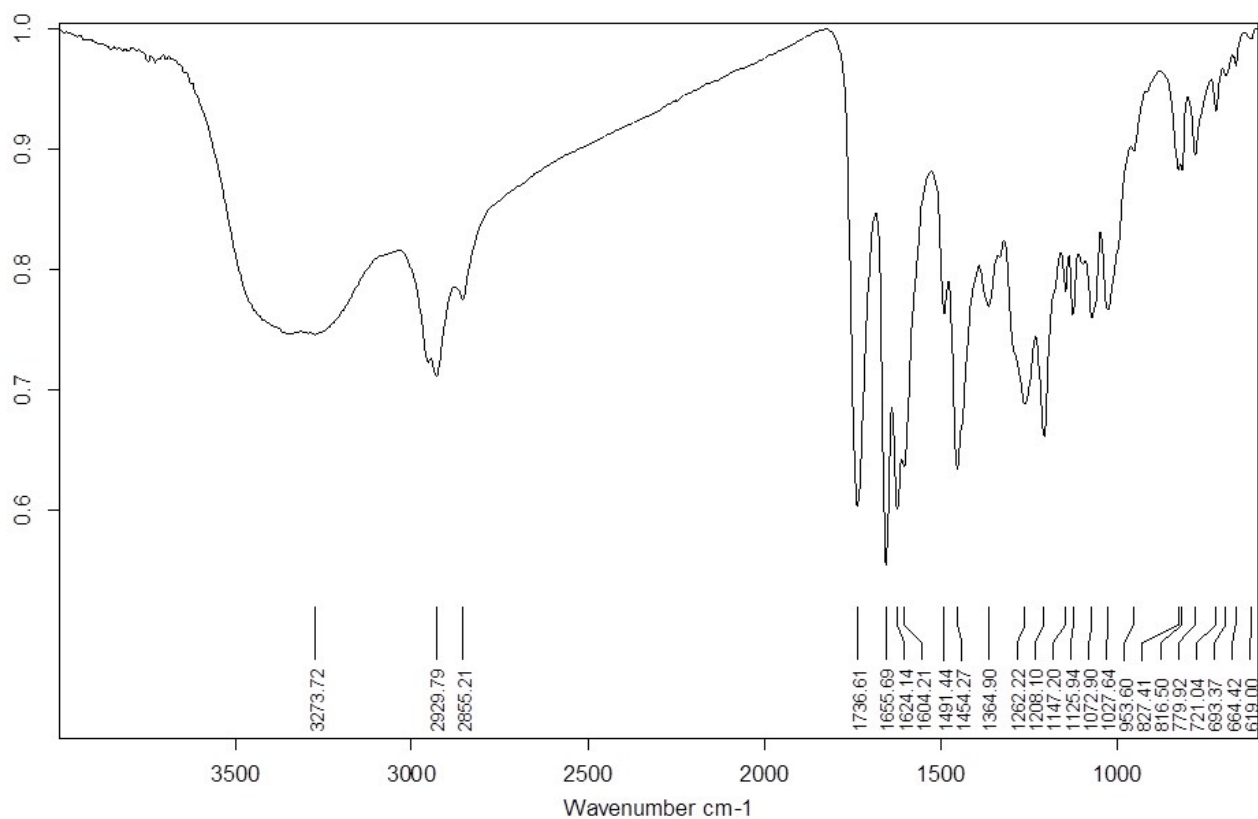


Figure S8. IR spectrum of **1** (on an ATR crystal).

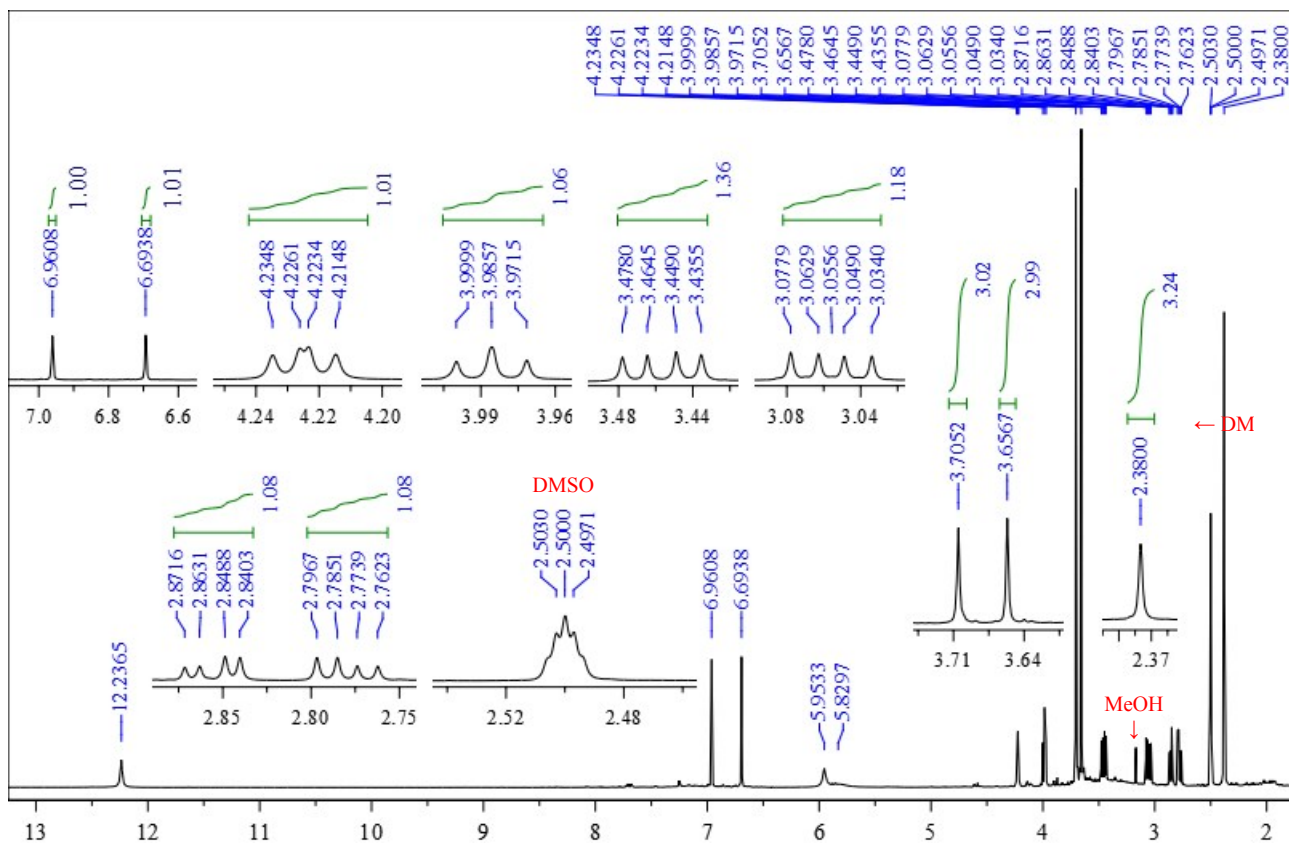


Figure S9. 600 MHz ^1H NMR spectrum of **1** in $\text{DMSO-}d_6$.

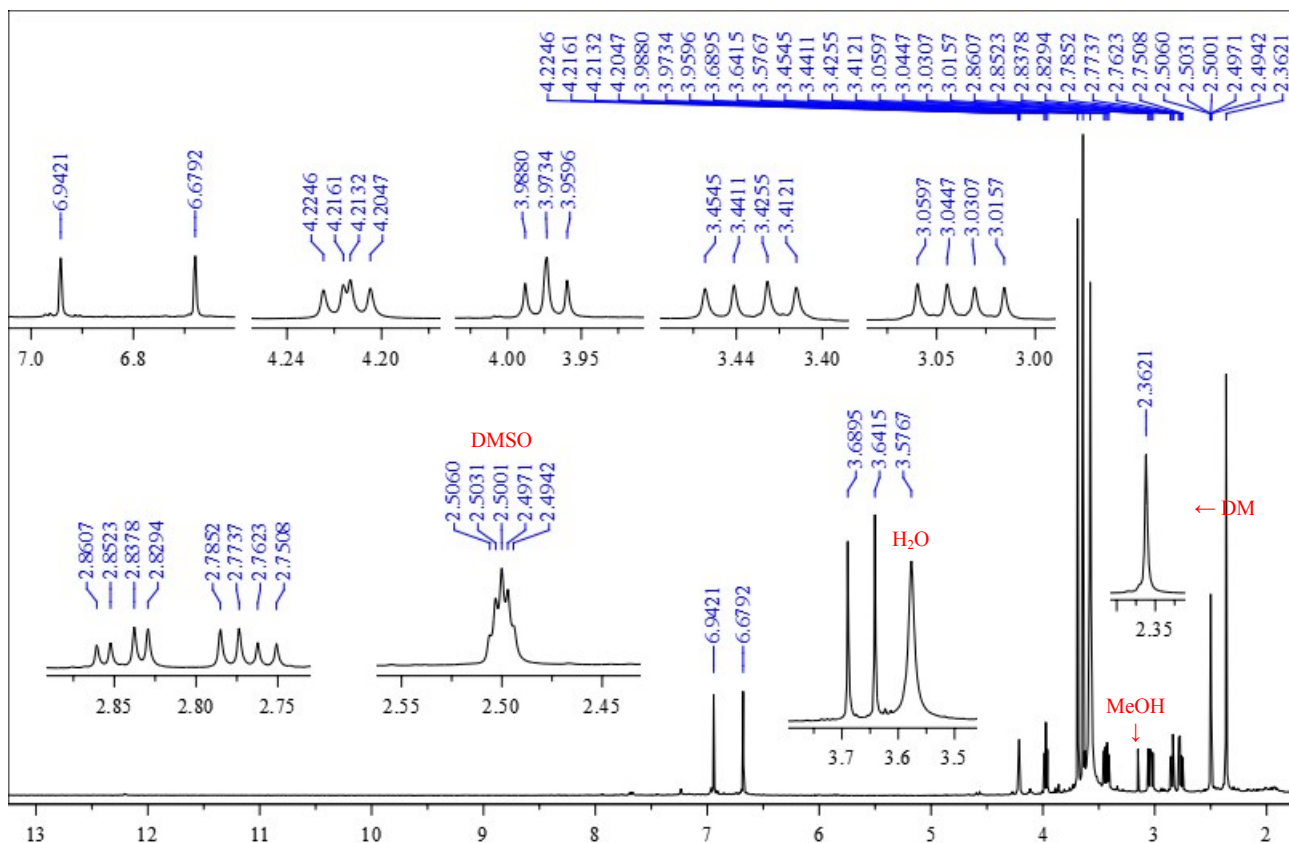


Figure S10. 600 MHz ^1H NMR spectrum of **1** in $\text{DMSO-}d_6$ after adding drops of D_2O .

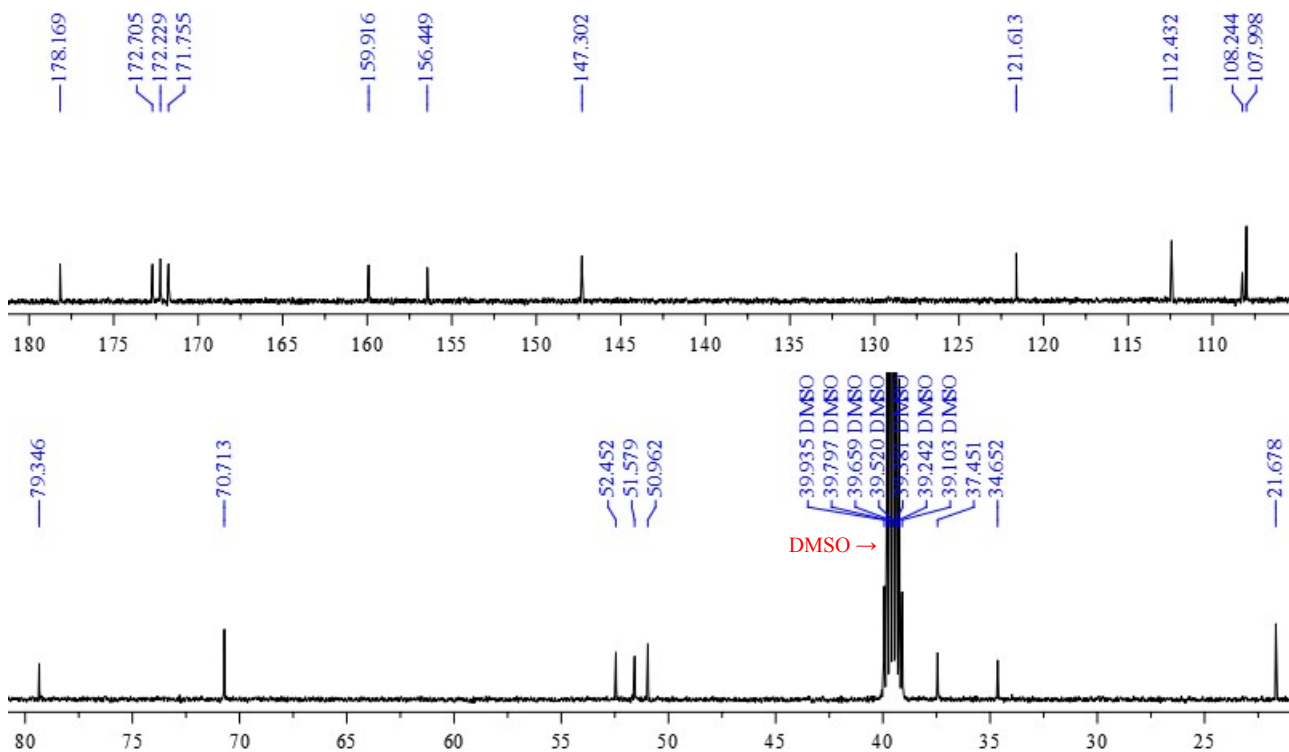
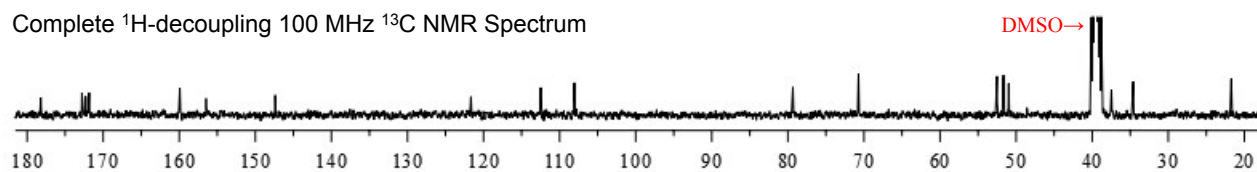


Figure S11. 150 MHz ^{13}C NMR spectrum of **1** in $\text{DMSO-}d_6$.

Complete ^1H -decoupling 100 MHz ^{13}C NMR Spectrum



100 MHz DEPT Spectra

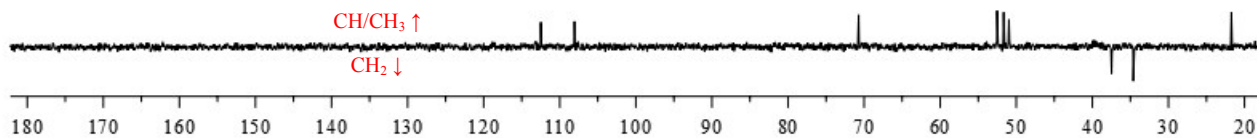
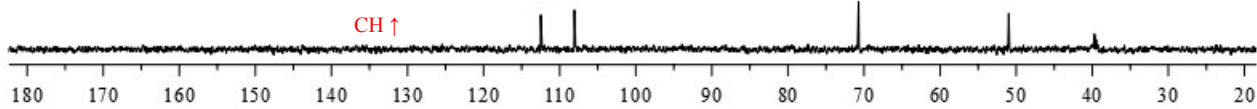
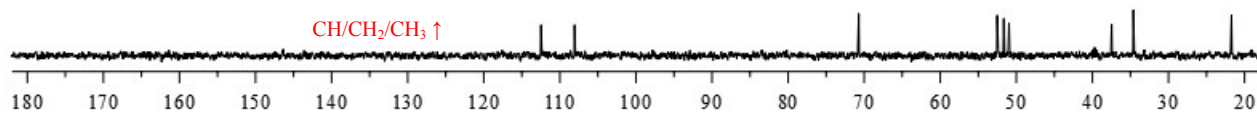


Figure S12. 100 MHz ^{13}C NMR and DEPT spectra of **1** in $\text{DMSO-}d_6$.

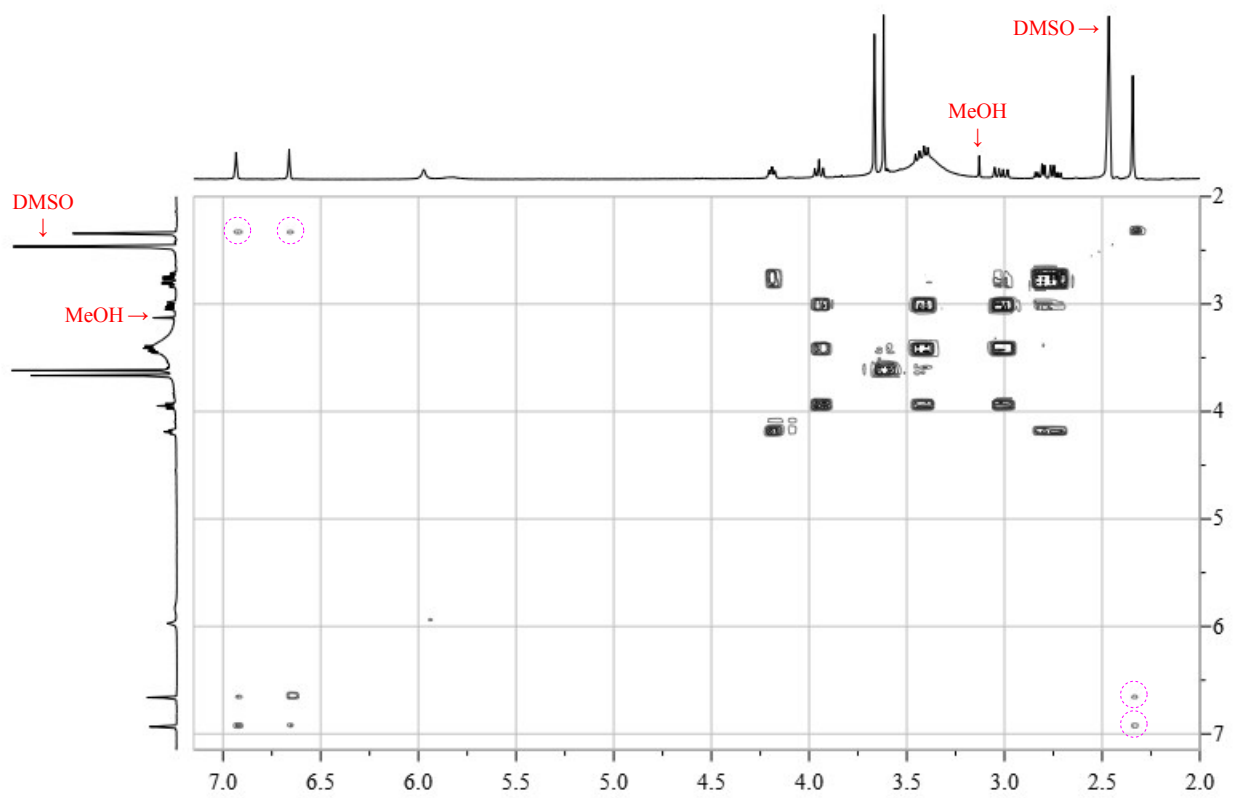


Figure S13. 400 MHz ^1H - ^1H COSY spectrum of **1** in $\text{DMSO-}d_6$.

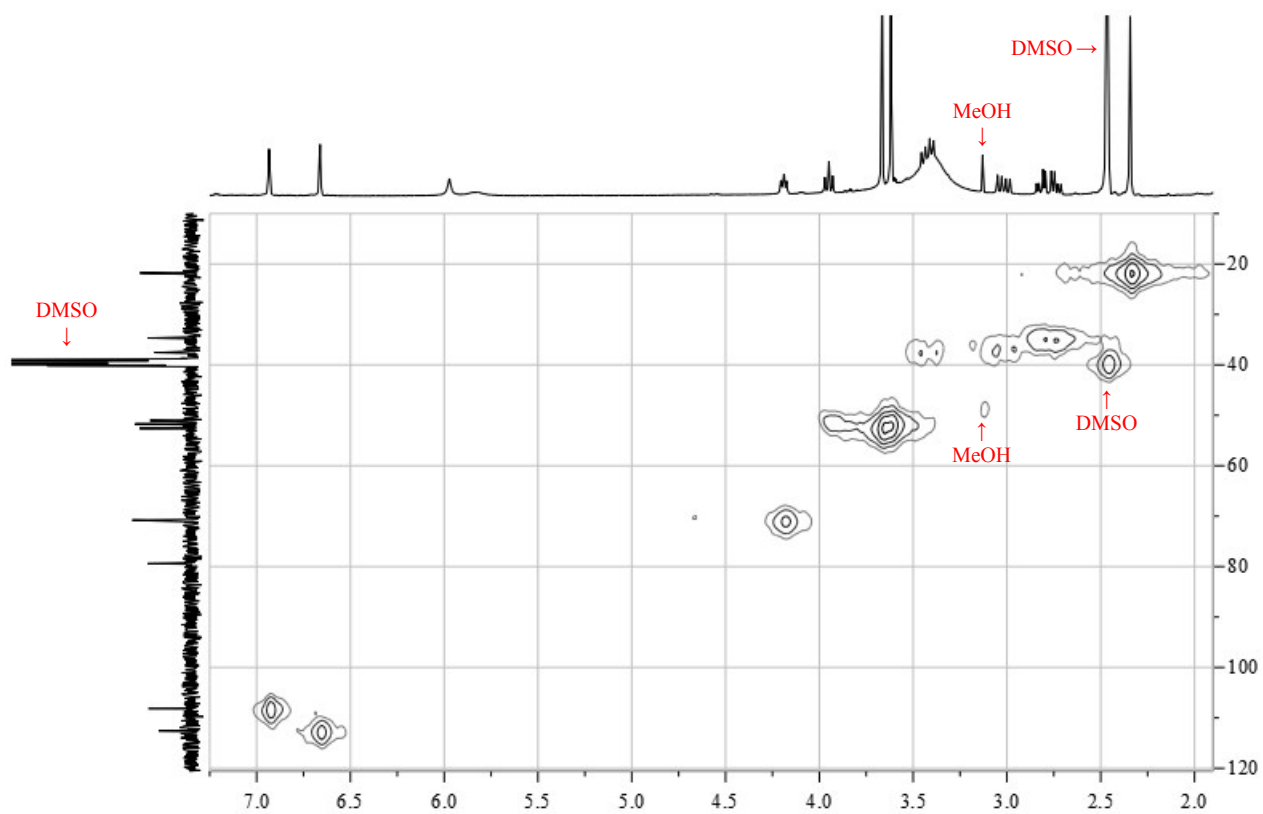


Figure S14. 400 MHz $^1\text{H}/100\text{ MHz } ^{13}\text{C}$ HMQC spectrum of **1** in $\text{DMSO-}d_6$.

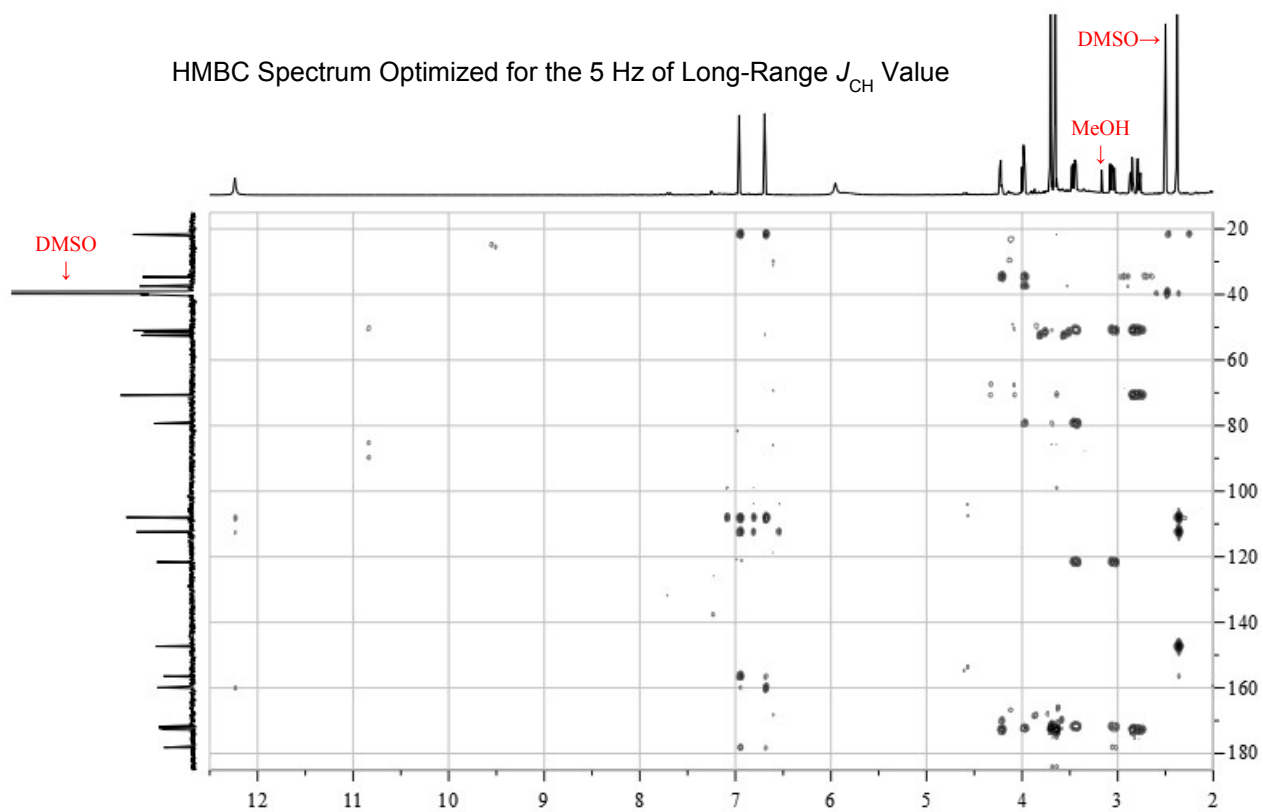


Figure S15. 600 MHz $^1\text{H}/150\text{ MHz } ^{13}\text{C}$ HMBC spectrum of **1** in $\text{DMSO-}d_6$.

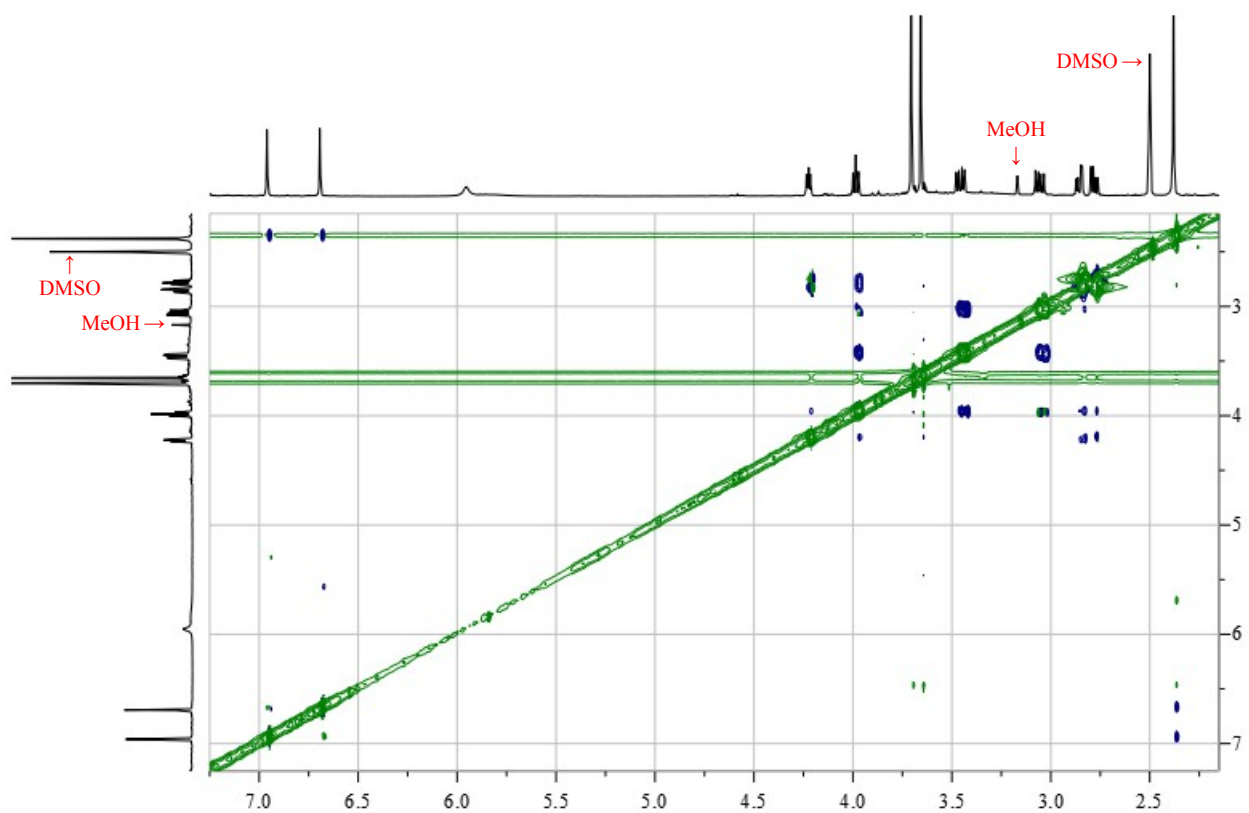


Figure S16. 600 MHz ROESY spectrum of **1** in DMSO- d_6 .

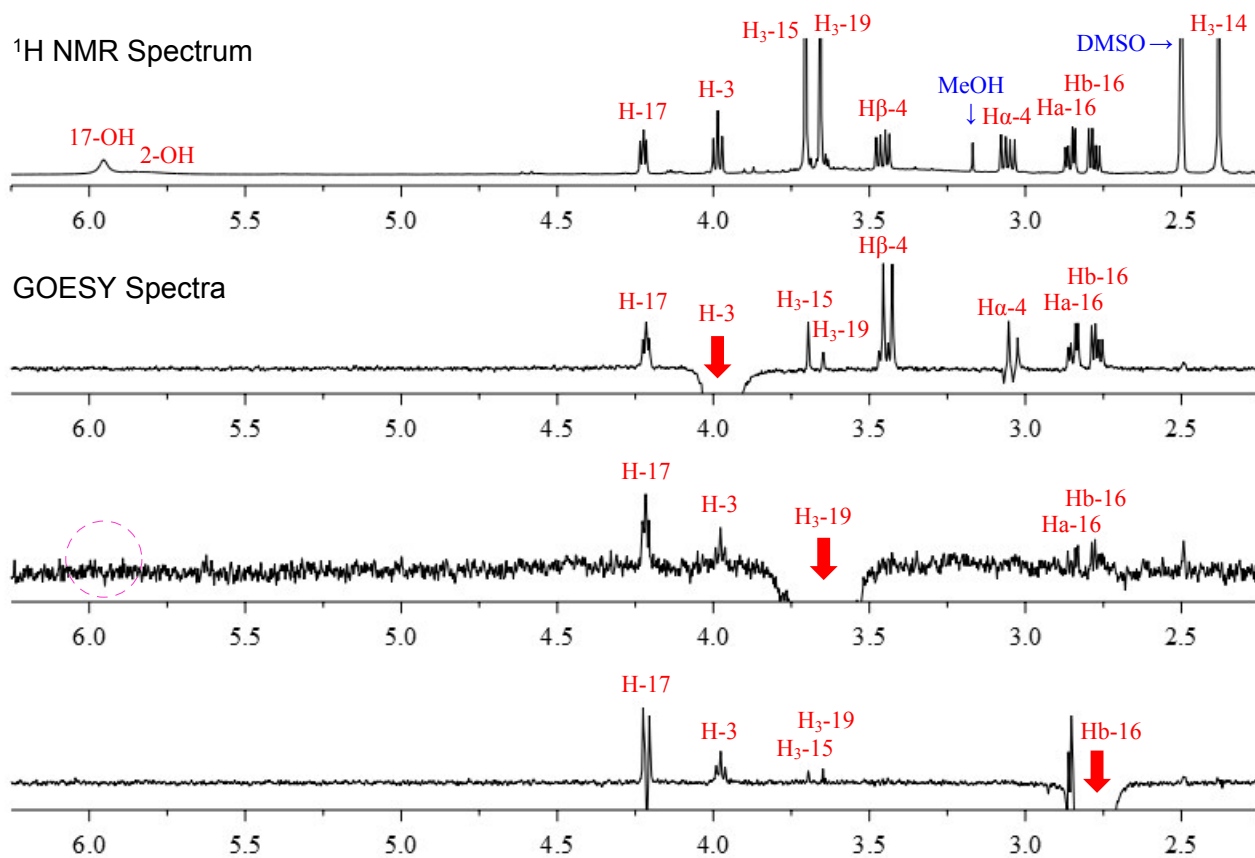


Figure S17. 600 MHz ^1H NMR and 1D GOESY spectra of **1** in DMSO- d_6 .